PHYSICAL REVIEW B VOLUME 58, NUMBER 10 1 SEPTEMBER 1998-II

Spin-wave gap and spin dynamics of γ-Mn alloys

R. S. Fishman
Solid State Division, Oak Ridge National Laboratory, Oak Ridge, Tennessee 37831-6032

S. H. Liu
Physics Department, University of California, San Diego, California 92093

(Received 13 February 1998)

The magnetic phase diagram of γ-Mn alloys contains both collinear and noncollinear magnetic phases in fct and fcc crystal structures. Using a two-band model which incorporates the magnetoelastic coupling, we find that the gap $\Delta_{sw}(T)$ in the spin-wave dispersion is proportional to the 3/2 power of the sublattice magnetization $M(T)$, in agreement with experiments on both the collinear and noncollinear magnetic phases. For the noncollinear magnetic phases observed in MnNi and FeMn alloys, high-frequency excitations are predicted with $\omega(\vec{q}=0)\sim\Delta$, where 2Δ is the energy gap in the quasiparticle spectrum. [S0163-1829(98)51834-6]

A remarkable diversity of collinear and noncollinear magnetic phases are supported by γ-Mn alloys. Since the fcc phase of pure Mn is only stable at very high temperatures, $\gamma-$Mn is commonly produced by doping with Fe, Ni, or Cu. Many such γ-Mn alloys undergo a lattice distortion below the Néel temperature T_N. Whereas moderately doped alloys become fct with $c<a$, the more heavily doped Fe_xMn_{1-x} [$x>45\%$ (Refs. 1 and 2)] and $Mn_{1-x}Ni_x$ [$x>22\%$ (Ref. 3)] alloys remain cubic with $c=a$. For a narrow impurity range between 17% and 22%, MnNi alloys become fct at low temperatures with $c>a$. According to the phenomenological model of Jo and Hirai,[4] these three crystal structures may be identified with the three magnetic phases sketched in Fig. 1. Such an identification has been substantially confirmed by band-structure calculations[5,6] and by experiments.[7,8] In this paper, we use a simple Hamiltonian which includes magnetoelastic interactions and two bands of quasiparticles to predict the spin excitations about the single (S), double (D), and triple (T) spin-density wave (SDW) phases of Fig. 1. For any of these magnetic phases, the gap $\Delta_{sw}(T)$ in the spin-wave spectrum is proportional to the 3/2 power of the sublattice magnetization $M(T)$. We also report the existence of high-frequency, collective spin excitations associated with the DSDW and TSDW phases.

Moderately doped γ-Mn alloys[2] have Néel temperatures close to 470 K and magnetic moments of about 2.3 μ_B. In all known γ-Mn alloys, the structural phase transitions[3] are either below or coincide with the Néel temperature, which strongly suggests the importance of magnetoelastic effects. The excitation spectra of both fct (Refs. 9 and 10) and fcc (Refs. 11 and 12) Mn alloys exhibit low-temperature energy gaps Δ_{sw} between 7 and 10 meV. Experimentalists[12–14] have reported that $\Delta_{sw}(T)$ is proportional to $M(T)^{\alpha}$, where $1.5\leqslant\alpha\leqslant1.83$. However, this temperature dependence has never been satisfactorily explained.

Formally, the SSDW, DSDW, and TSDW phases may be written as

$$\mathbf{S}_i=M\hat{z}\,\cos(\mathbf{Q}_z\cdot\mathbf{R}_i), \tag{1}$$

$$\mathbf{S}_i=\frac{1}{\sqrt{2}}M[\hat{x}\,\cos(\mathbf{Q}_x\cdot\mathbf{R}_i)+\hat{y}\,\cos(\mathbf{Q}_y\cdot\mathbf{R}_i)], \tag{2}$$

$$\mathbf{S}_i=\frac{1}{\sqrt{3}}M[\hat{x}\,\cos(\mathbf{Q}_x\cdot\mathbf{R}_i)+\hat{y}\,\cos(\mathbf{Q}_y\cdot\mathbf{R}_i)+\hat{z}\,\cos(\mathbf{Q}_z\cdot\mathbf{R}_i)], \tag{3}$$

where $\mathbf{Q}_x=2\pi\hat{x}/a$, $\mathbf{Q}_y=2\pi\hat{y}/a$, $\mathbf{Q}_z=2\pi\hat{z}/c$, and $\cos(\mathbf{Q}_\gamma\cdot\mathbf{R}_i)=\pm1$. In Eqs. (1)–(3), the sharply peaked Bloch wave functions of the *d*-band electrons have been replaced by delta functions. The DSDW and TSDW phases are often grouped together as multiple (M) SDW's. For the TSDW of Eq. (3), the spin points along the (1,1,1), (1,1,$\bar{1}$), (1,$\bar{1}$,1), and ($\bar{1}$,1,1) directions. Unlike the SSDW and DSDW phases, the TSDW does not violate cubic symmetry and is consistent with the magnetic fcc phase of FeMn and MnNi alloys. This phase may also occur in the fcc compound USb.[15,16]

The band structure of γ-Mn alloys[17] contains a large electron Fermi surface *a* centered at the Γ point and large hole Fermi surfaces *b* at the six neighboring *X* points. Unlike the more closely nested Fermi surfaces of Cr alloys,[18] the Fermi surfaces of γ-Mn alloys are sufficiently different in shape that incommensurate SDW ordering is not possible. The commensurate SDW's constructed above are produced by the Coulomb attraction *U* between the electrons and holes on

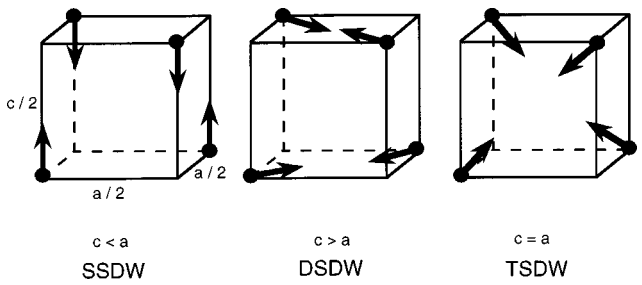

FIG. 1. The single, double, and triple SDW phases which are stabilized in different crystal structures.

the a and b Fermi surfaces. Our Hamiltonian also includes the magnetoelastic interaction between the spin and the lattice:

$$H = H_0 + H_{coul} + H_{me}, \tag{4}$$

$$H_0 = \sum_{\mathbf{k},\alpha} [\epsilon_a(\mathbf{k}) a^\dagger_{\mathbf{k}\alpha} a_{\mathbf{k}\alpha} + \epsilon_b(\mathbf{k}) b^\dagger_{\mathbf{k}\alpha} b_{\mathbf{k}\alpha}], \tag{5}$$

$$H_{coul} = \frac{U}{V} \sum_{\mathbf{q},\mathbf{k},\mathbf{k}',\alpha,\beta} a^\dagger_{\mathbf{k}\alpha} b^\dagger_{\mathbf{k}'\beta} b_{\mathbf{k}'+\mathbf{q}\beta} a_{\mathbf{k}-\mathbf{q}\alpha}, \tag{6}$$

$$H_{me} = V\Bigg(\frac{1}{2} c_{11}(\epsilon_{xx}^2 + \epsilon_{yy}^2 + \epsilon_{zz}^2) + c_{12}(\epsilon_{xx}\epsilon_{yy} + \epsilon_{yy}\epsilon_{zz} + \epsilon_{zz}\epsilon_{xx}) + \frac{g}{N}\sum_i (S_{ix}^2 \epsilon_{xx} + S_{iy}^2 \epsilon_{yy} + S_{iz}^2 \epsilon_{zz})\Bigg), \tag{7}$$

where $a^\dagger_{\mathbf{k}\alpha}$ and $b^\dagger_{\mathbf{k}\alpha}$ are the creation operators for electrons on the a and b bands. The strain components are given by ϵ_{ii}, c_{11} and c_{12} are the elastic constants, and g is the magnetoelastic coupling strength. In terms of the Fermi operators, the spin operator is defined by

$$S_{i\gamma} = \frac{1}{2}\sum_{\alpha,\beta} (a^\dagger_{i\alpha} + b^\dagger_{i\alpha}) \sigma^\gamma_{\alpha\beta} (a_{i\beta} + b_{i\beta}), \tag{8}$$

where $\underline{\sigma}^\gamma$ are the Pauli matrices.

After minimizing the Hamiltonian with respect to the strain components, it is easy to show that the average strain for each SDW configuration corresponds to the crystal structures identified by Jo and Hirai[4] in Fig. (1). To proceed further, we use the mean-field approximation to replace H_{me} with

$$H'_{me} = -\sum_i \mathbf{B}_i \cdot \mathbf{S}_i + \text{ const}, \tag{9}$$

where the effective field $\mathbf{B}_i$ is given by

$$\mathbf{B}_i = -2\frac{V}{N} g[\epsilon_{xx}\langle S_{ix}\rangle \hat{x} + \epsilon_{yy}\langle S_{iy}\rangle \hat{y} + \epsilon_{zz}\langle S_{iz}\rangle \hat{z}]. \tag{10}$$

For each magnetic phase, $\mathbf{B}_i$ is parallel to $\mathbf{S}_i$. Since the strain components ϵ_{ii} are proportional to M^2, $\mathbf{B}_i$ is proportional to M^3. Within this approximation, every electron and hole independently experiences the effective field $\mathbf{B}_i$ exerted by the magnetoelastic interaction. For each of the three SDW phases, the interaction constant κ is defined in terms of c_{11}, c_{12}, and g through the relation $\langle H'_{me}\rangle = -N\kappa M^4$. When κ exceeds a critical value κ_c, the magnetic and structural phase transitions become first order. Such a martensitic transformation[19] may be induced by the softening of a lattice phonon and the resulting enhancement of κ.

It is now straightforward to use the random-phase approximation (RPA) to formulate the equations of motion for the Fermi operators and for the imaginary time Green's functions

$$G(\mathbf{k},\tau)_{\alpha\beta,aa} = -\langle T_\tau a_{\mathbf{k}\alpha}(\tau) a^\dagger_{\mathbf{k}\beta}(0)\rangle = \delta_{\alpha\beta} G(\mathbf{k},\tau)_{aa}, \tag{11}$$

$$G(\mathbf{k},\tau)^\gamma_{\alpha\beta,bb} = -\langle T_\tau b_{\mathbf{k}+\mathbf{Q}_\gamma\alpha}(\tau) b^\dagger_{\mathbf{k}+\mathbf{Q}_\gamma\beta}(0)\rangle = \delta_{\alpha\beta} G(\mathbf{k},\tau)_{bb}, \tag{12}$$

$$G(\mathbf{k},\tau)^{\gamma\gamma'}_{\alpha\beta,bb'} = -\langle T_\tau b_{\mathbf{k}+\mathbf{Q}_\gamma\alpha}(\tau) b^\dagger_{\mathbf{k}+\mathbf{Q}_{\gamma'}\beta}(0)\rangle = (\sigma^\gamma \cdot \sigma^{\gamma'})_{\alpha\beta} G(\mathbf{k},\tau)_{bb'}, \quad \gamma \neq \gamma' \tag{13}$$

$$G(\mathbf{k},\tau)^\gamma_{\alpha\beta,ab} = -\langle T_\tau a_{\mathbf{k}\alpha}(\tau) b^\dagger_{\mathbf{k}+\mathbf{Q}_\gamma\beta}(0)\rangle = \sigma^\gamma_{\alpha\beta} G(\mathbf{k},\tau)_{ab}. \tag{14}$$

In Eqs. (12)–(14), $G(\mathbf{k},\tau)_{bb}$, $G(\mathbf{k},\tau)_{bb'}$, and $G(\mathbf{k},\tau)_{ab}$, are independent of γ provided that the hole band b has cubic symmetry about X so that $\epsilon_b(\mathbf{k}+\mathbf{Q}_\gamma) \equiv \epsilon_{b+}(\mathbf{k})$ does not depend on γ. Due to the size difference between the electron and hole Fermi surfaces, there is an energy mismatch $\epsilon_{b+}(\mathbf{k}) - \epsilon_a(\mathbf{k}) = z_0/2$ at the Fermi momentum $\mathbf{k}_F$ of the a Fermi surface.

After solving for the Green's functions, we find that the off-diagonal Green's function G_{ab} is responsible for the appearance of an energy gap $2\Delta(T)$ among the hybridized a and b quasiparticle energies. Remarkably, $\Delta(T)$ is identical in all three magnetic phases:

$$\Delta(T) = \frac{N}{2V} UM(T) + 2\kappa M(T)^3, \tag{15}$$

which is enhanced by the magnetoelastic interaction. The energy gap 2Δ may be inferred from the activation of the electrical resistivity or obtained directly from photoemission measurements. For a typical γ-Mn alloy with $T_N \approx 450$ K, $2\Delta(0)$ should be about 100 meV, which is an order of magnitude larger than the SW gap $\Delta_{sw}(0)$. However, because of their disparate shapes, large portions of the a and b Fermi surfaces will not be gapped.

The RPA for the spin correlation functions is quite similar in all three SDW phases, except that different $\mathbf{Q}_\gamma$ are coupled in the MSDW phases,[20] in particular through the Green's function $G(\mathbf{k},\tau)_{bb'}$ defined above. We solve for the excitation spectrum after restricting the wave vector $\mathbf{q}$ to lie parallel to one of the ordering wave vectors $\mathbf{Q}_\gamma$.

For the S ($m=1$), D ($m=2$), and T ($m=3$) SDW phases, spin-wave (SW) excitations about the magnetic satellite $\mathbf{Q}_\gamma$ are given by the zeroes of the function $1 - U[\chi_1(\mathbf{q},\omega) - m\chi_2(\mathbf{q},\omega)]$, where

$$\chi_1(\mathbf{q},\omega) = -\frac{T}{V}\sum_{\mathbf{k},l} G(\mathbf{k}, i\nu_l)_{aa,bb'} [G(\mathbf{k}+\mathbf{q}, i\nu_l - i\omega_n) + (m-1) G(\mathbf{k}+\mathbf{q}, i\nu_l - i\omega_n)_{bb'}]\Big|_{i\omega_n \to \omega + i\varepsilon^+}, \tag{16}$$

$$\chi_2(\mathbf{q},\omega) = -\frac{T}{V}\sum_{\mathbf{k},l} G(\mathbf{k}, i\nu_l)_{ab} G(\mathbf{k}+\mathbf{q}, i\nu_l - i\omega_n)_{ab}\Big|_{i\omega_n \to \omega + i\varepsilon^+}, \tag{17}$$

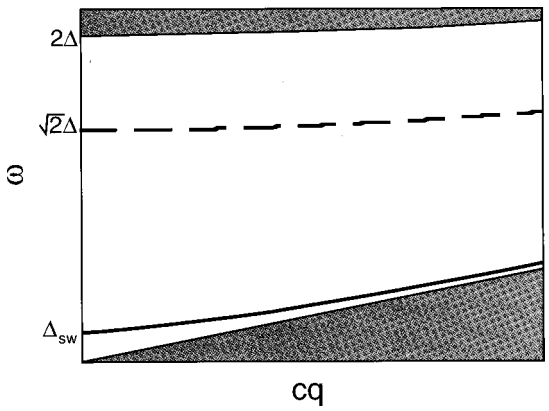

FIG. 2. The SW (solid) and high-frequency collective (dashed) modes of γ-Mn. The shaded regions contains single-particle excitations.

and $\mathbf{q}$ is measured $\mathbf{Q}_\gamma$. Here, $\nu_l=(2l+1)\pi T$ and $\omega_n=2n\pi T$ are Matsubara frequencies.

Because the magnetoelastic interaction violates rotational symmetry, the SW spectrum contains an energy gap $\Delta_{\rm sw}(T)$, which is formally the same in all three magnetic phases. Near the Néel temperature, it is explicitly given by

$$\Delta_{\rm sw}(T)=\frac{16}{\sqrt{2\pi}}\sqrt{\frac{\kappa T_{\rm N}}{\rho_{eh}U}}\cosh\left(\frac{z_0}{8T_{\rm N}}\right)M(T)^{3/2}, \qquad (18)$$

where ρ_{eh} is the two-spin density-of-states of the electron and hole Fermi surfaces. Consequently, the spin-wave gap is proportional to the $\alpha=3/2$ power of the sublattice magnetization and grows with the mismatch z_0 between the Fermi surfaces. A power law of $\alpha=2$ would be obtained from a local-moment description of γ-Mn based on the Heisenberg model with $\epsilon_{ii}\propto M(T)^2$. By contrast, Sato and Maki[21] used a two-band RPA to predict that $\alpha=1$, which would follow from a Heisenberg model with temperature-independent strain.[22] While Tajima *et al.*[12] observed a 3/2 power dependence for three different fcc FeMn alloys, more recent studies of fct MnCu (Ref. 13) and MnNi (Ref. 14) alloys find power laws with $\alpha=1.56$ and 1.83, respectively. However, the statistics of the latter study are not convincing.

For small κ, the SW dispersion may be closely approximated by $\omega_{\rm sw}(\mathbf{q})=\sqrt{\Delta_{\rm sw}^2+(cq)^2}$, where the SW velocity c is proportional to the Fermi velocity. This dispersion is sketched in Fig. 2, where single-particle excitations occupy the shaded portions. So the SW modes are undamped within the RPA. Experimentally, the SW modes are damped with a width proportional to the wave vector q.[9,12] This damping may be produced either by impurity scattering or by the decay of SW's into single-particle excitations of the nongapped portions of the Fermi surface.

Due to the coupling between different $\mathbf{Q}_\gamma$, a MSDW supports an additional class of collective excitations given by the zeros of $1-U\chi_3(\mathbf{q},\omega)$, where

$$\chi_3(\mathbf{q},\omega)=-\frac{T}{V}\sum_{\mathbf{k},l} G(\mathbf{k},i\nu_l)_{aa}[G(\mathbf{k}+\mathbf{q},i\nu_l-i\omega_n)_{bb} - G(\mathbf{k}+\mathbf{q},i\nu_l-i\omega_n)_{bb'}]|_{i\omega_n\to\omega+i\varepsilon^+}. \qquad (19)$$

For a MSDW, only $1/m$ of the holes on each of the m nested hole Fermi surfaces (connected by $\mathbf{Q}_\gamma$ from each electron Fermi surface) participates in the SDW condensate. The remaining holes have energies which are unperturbed by the SDW. This additional class of collective excitations is produced by the Coulomb attraction between the noninteracting holes and the paired electrons on the a Fermi surface. By contrast with the SW modes, all of these additional modes are damped within our model. For $z_0=0$, one such collective mode has the frequency $\omega_c(\mathbf{q}=0)=\sqrt{2}\Delta$, as sketched in Fig. 2. For $\Delta\approx 50$ meV, ω_c should be close to 70 meV. A more detailed discussion of these collective modes will be presented elsewhere.[20]

Such a high-frequency mode may have been observed below the Néel temperature $T_{\rm N}=240$ K of USb,[15] where a TSDW phase was conjectured and modeled by Jensen and Bak.[16] Within their local-moment description, the high-frequency collective mode with $\omega_c\approx 30$ meV is a geometric consequence of the TSDW structure.

A spallation source could be used to probe these collective excitations in the DSDW and TSDW phases of γ-Mn alloys. Though their frequencies are identical in the MSDW phases, these collective excitations have a larger intensity in the TSDW phase. On the other hand, the SW modes should be less intense in the TSDW phase. Hence, it might be interesting to study the change in intensity of these magnetic excitations as the temperature falls through the fcc (TSDW) to fct (DSDW) transition[3] in $Mn_{1-x}Ni_x$ alloys with $0.17<x<0.22$.

To summarize, we have studied the spin excitations about the three magnetic phases of γ-Mn alloys. While a SW mode with energy gap proportional to $M(T)^{3/2}$ was found in all three magnetic states, high-frequency collective modes are predicted for the two MSDW states.

This research was supported by Oak Ridge National Laboratory, which is managed by Lockheed Martin Energy Research Corp. for the U.S. Department of Energy under Contract No. DE-AC05-96OR22464.

[1] J. S. Kouvel and J. S. Kasper, J. Phys. Chem. Solids **24**, 529 (1963).

[2] Y. Endoh and Y. Ishikawa, J. Phys. Soc. Jpn. **30**, 1614 (1971).

[3] N. Honda, Y. Tanji, and Y. Nakagawa, J. Phys. Soc. Jpn. **41**, 1931 (1976).

[4] T. Jo and K. Hirai, J. Phys. Soc. Jpn. **55**, 2017 (1986).

[5] T. Takahashi, T. Ukai, and N. Mori, J. Appl. Phys. **63**, 3611 (1988).

[6] S. Fujii, S. Ishida, and S. Asano, J. Phys. Soc. Jpn. **60**, 4300 (1991).

[7] S. J. Kennedy and T. J. Hicks, J. Phys. F **17**, 1599 (1987).
[8] S. Kawarazaki *et al.*, Phys. Rev. Lett. **61**, 471 (1988).
[9] M. C. K. Wiltshire, M. M. Elcombe, and C. J. Howard, J. Phys. F **15**, 1595 (1985).
[10] J. A. Fernandez-Baca *et al.*, J. Magn. Magn. Mater. **104-107**, 699 (1992).
[11] Y. Endoh *et al.* Solid State Commun. **13**, 1179 (1973).
[12] K. Tajima *et al.*, J. Phys. Soc. Jpn. **41**, 1195 (1976).
[13] K. Mikke, J. Jankowska-Kisienlinska, and E. Jaworska, Physica B **180&181**, 247 (1992).
[14] J. Jankowska-Kisielinska, K. Mikke, and J. J. Milczarek, J. Phys.: Condens. Matter **9**, 10761 (1997).
[15] G. H. Lander and W. G. Stirling, Phys. Rev. B **21**, 436 (1980).
[16] J. Jensen and P. Bak, Phys. Rev. B **23**, 6180 (1981).
[17] J. Yamashita, S. Asano, and S. Wakoh, J. Appl. Phys. **39**, 1274 (1968).
[18] P. A. Fedders and P. C. Martin, Phys. Rev. **143**, 245 (1966).
[19] Y. Tsunoda and N. Wakabayashi, J. Phys. Soc. Jpn. **50**, 3341 (1981).
[20] R. S. Fishman and S. H. Liu (unpublished).
[21] H. Sato and K. Maki, Prog. Theor. Phys. **55**, 319 (1976).
[22] See, for example, K. Yosida, *Theory of Magnetism* (Springer, Berlin, 1991).